



Production of heavy trans-target nuclei in multinucleon transfer reactions

V. I. Zagrebaev¹ and Walter Greiner²

¹*Flerov Laboratory of Nuclear Reactions, JINR, Dubna, Moscow Region, Russia*

²*Frankfurt Institute for Advanced Studies, Johann Wolfgang Goethe-Universität, Frankfurt, Germany*

(Received 18 January 2013; revised manuscript received 22 February 2013; published 6 March 2013)

Problems of production and study of new neutron-enriched heavy nuclei are discussed. Low-energy multinucleon transfer reactions are shown to be quite appropriate for this purpose. Reactions with actinide beams and targets are of special interest for synthesis of new neutron-enriched transfermium nuclei and not-yet-known nuclei with closed neutron shell $N = 126$ having the largest impact on the astrophysical r-process. The estimated cross sections for the production of these nuclei look very promising for planning such experiments at currently available accelerators. These experiments, however, are rather expensive and difficult to perform because of low intensities of the massive projectile beams and problems of separating and detecting the heavy reaction products. Thus, realistic predictions of the corresponding cross sections for different projectile-target combinations are definitely required. Some uncertainty still remains in the values of several parameters used for describing the low-energy nuclear dynamics. This uncertainty does not allow one to perform very accurate predictions for the productions of new heavier-than-target (trans-target) nuclei in multinucleon transfer reactions. Most of these parameters (nucleon transfer rate, nuclear viscosity, and fission barriers) are fundamental characteristics of low-energy nuclear dynamics. Determination of the values of these parameters (as well as their temperature dependence) is of significance in its own right. The available experimental data on the production of heavy nuclei in low-energy multinucleon transfer reactions are still insufficient and fragmentary. Several new experiments are proposed, these include those in which the role of shell effects in reaction dynamics can be better clarified.

DOI: [10.1103/PhysRevC.87.034608](https://doi.org/10.1103/PhysRevC.87.034608)

PACS number(s): 25.70.Jj, 27.90.+b

I. MOTIVATION

Thirty years ago there had been a great deal of interest in the use of heavy-ion multinucleon transfer reactions with actinide targets to produce new neutron-rich isotopes of heavy and superheavy (SH) nuclei. Many such experiments were performed during those times [1–7] and very interesting information concerning collision dynamics have been derived. The cross sections for production of above-target elements were found to decrease very rapidly with increasing atomic number of surviving heavy nuclei. Nevertheless, the cross section level of $0.1 \mu\text{b}$ had been reached, and several isotopes of Fm and Md have been synthesized in low-energy collisions of ^{238}U with a ^{248}Cm target [5]. It was found that the yields of near- and above-target actinide nuclei depend strongly on the choice of the projectile nucleus [6]. Nuclear structure effects (in particular, the closed neutron shell $N = 126$) were also observed in the distribution of binary reaction products formed in low-energy dissipative collisions of heavy ions [8].

Renewed interest in multinucleon transfer reactions with heavy ions has arisen because of the limitations of other reaction mechanisms for the production of new heavy and SH nuclei. It is well known that for the elements with $Z > 100$ only neutron-deficient isotopes (located to the left of the stability line) have been synthesized so far. The “northeast” area of the nuclear map cannot be reached in the fusion, fission, or fragmentation processes widely used nowadays for the production of new nuclei. Multinucleon transfer processes in near-barrier collisions of heavy (and very heavy, U-like) ions seem to be the only reaction mechanism (besides the multiple neutron capture process [9]) allowing us to produce and explore neutron-rich heavy nuclei including those located at the SH island of stability.

In our recent study we found that shell effects may give us a gain in the yields of heavy neutron-rich nuclei formed in multinucleon transfer reactions [10–13]. In particular, the cross section for the production of unknown neutron-rich nuclei located below ^{208}Pb along the closed neutron shell $N = 126$ were predicted to be of the order of several microbarns in low-energy collisions of ^{136}Xe or ^{192}Os with a ^{208}Pb target. Rather optimistic predictions were obtained also for the production of SH nuclei. For near-barrier collisions of ^{238}U with ^{248}Cm cross sections higher than 1 pb have been predicted for the production of new neutron-enriched isotopes of elements with $Z \leq 106$ located already at the stability line or even beyond it.

These are the shell effects which may significantly enhance the yield of SH nuclei for appropriate projectile-target combinations. In Fig. 1 the charge and mass distributions of heavy primary reaction fragments are shown for near-barrier collisions of ^{48}Ca and ^{238}U with a curium target. The “lead peak” manifests itself in both reactions. However, for $^{48}\text{Ca} + ^{248}\text{Cm}$ collisions it corresponds to the conventional (symmetrizing) quasi-fission process in which nucleons are transferred mainly from a heavy target (here being ^{248}Cm) to a lighter projectile. This is a well-studied process both experimentally [14] and theoretically [15,16]. It is caused just by shell effects leading to a deep lead valley on the multidimensional potential energy surface which regulates the dynamics of the heavy nuclear system at low excitation energies.

Contrary to this conventional quasi-fission phenomena, in low-energy collisions of ^{238}U with a ^{248}Cm target nucleons may predominantly move from the lighter partner (here being uranium) to the heavy one, i.e., U transforms to a Pb-like nucleus and Cm to a complementary SH nucleus. In this case,

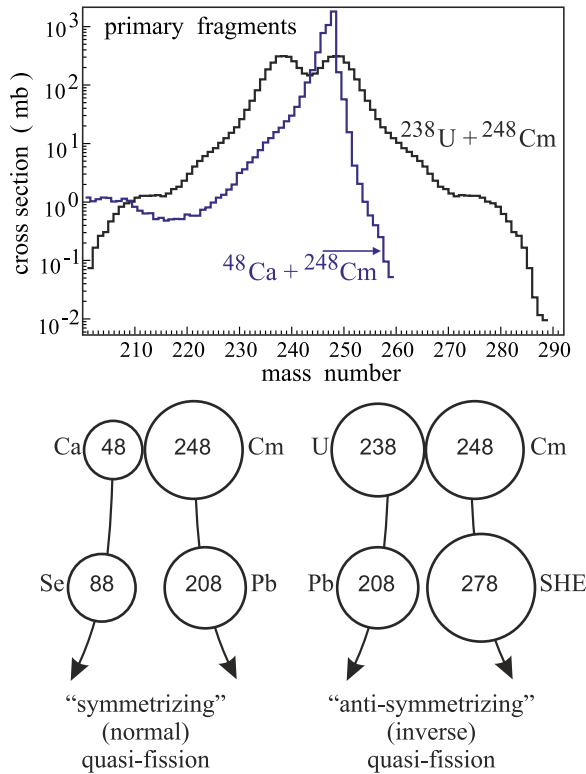


FIG. 1. (Color online) Calculated mass distributions of heavy primary reaction fragments formed in collisions of ^{48}Ca and ^{238}U with a ^{248}Cm target at $E_{c.m.} = 220$ and 770 MeV, correspondingly. Schematic views of conventional and “inverse” quasi-fission processes are also shown.

the appearance of the lead shoulder in the mass and charge distributions of the reaction fragments automatically leads to a pronounced shoulder in the region of SH nuclei (see Fig. 1). We called this the “inverse” (antisymmetrizing) quasi-fission process [10]. This process may really lead to enhanced yields of above-target nuclides, whereas even for rather heavy projectiles (such as ^{136}Xe) the nuclear system has a dominating symmetrizing trend of formation of reaction fragments with intermediate (heavier than projectile and lighter than target) masses (see Fig. 2).

A possibility for the production of new heavy neutron-rich nuclei in low-energy multinucleon transfer reactions is under discussion currently in several laboratories (see, for example, [17,18]). It is rather difficult to perform such experiments because of the low cross sections, the low intensities of these massive projectile beams, and the problems of detecting the reaction products. In this connection, realistic predictions of the corresponding cross sections for different projectile-target combinations are required as well as test experiments which may confirm or disprove these predictions.

Some time ago a test (surrogate to $\text{U} + \text{Cm}$) reaction of $^{160}_{64}\text{Gd}_{N=96} + ^{186}_{74}\text{W}_{N=112}$ was proposed [19], in which the same “inverse” quasi-fission process was expected due to neutron closed shells $N = 82$ and $N = 126$ located from the outside of the colliding partners. Recently, such an experiment has been performed [20]. Predicted and observed mass distributions of

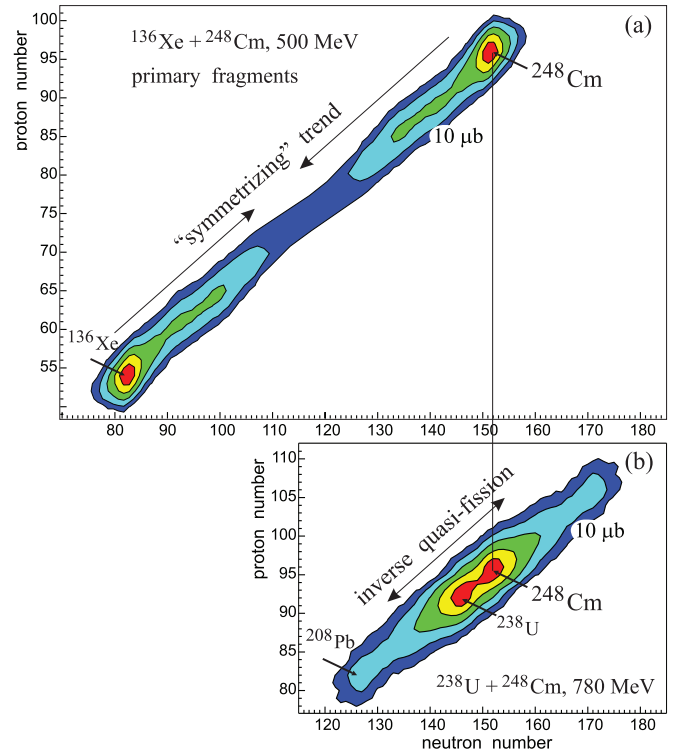


FIG. 2. (Color online) Landscapes of the calculated cross sections for the production of primary reaction fragments in collisions of ^{136}Xe (a) and ^{238}U (b) with a ^{248}Cm target at $E_{c.m.} = 500$ and 780 MeV, correspondingly. (Contour lines are drawn over one order of magnitude.)

targetlike nuclides formed in this reaction at $E_{c.m.} = 460$ MeV are shown in Fig. 3.

A pronounced shoulder (as compared with the conventional liquid drop model for the potential energy surface used for the calculation of nucleon transfer) has been predicted for the yields of trans-target nuclei (see the thick histogram in Fig. 3). Experimental data testify that the shell effects in low-energy multinucleon transfer reactions could be even stronger than expected. Cross sections for transfer of more than 15 nucleons from the lighter projectile to the heavier target were found to be higher than 20 mb. Unfortunately, the experimental technique (catcher foils + off-line radiochemistry) did not allow the experimenters to measure the yields of stable (as well as short-lived) isotopes and to reach the region of expected decrease of the cross sections for the production of translead nuclei (see Fig. 3).

Two other reactions, in which experimental cross sections for the production of trans-target nuclei exceed theoretical predictions, are the near-barrier reactions of ^{64}Ni [21] and ^{136}Xe [22] with a lead target. The calculated and measured cross sections for these reactions are shown in Figs. 4 and 5. In contrast to the previous case, here the shell effects (magic target and semi-magic projectiles) suppress nucleon transfer, and a monotonic decrease of the cross sections is expected with increasing number of transferred nucleons.

As can be seen from Figs. 4 and 5 experimental yields of Rn ($Z = 86$), Fr ($Z = 87$), and Ra ($Z = 88$) isotopes in the

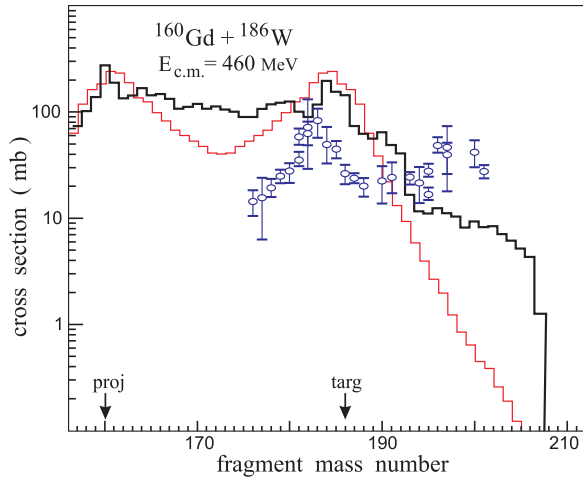


FIG. 3. (Color online) Predicted [19] and observed [20] mass distributions of reaction fragments (with energy loss higher than 15 MeV) formed in collisions of ^{160}Gd with ^{186}W at $E_{c.m.} = 460$ MeV. Experimental data are shown only for targetlike fragments. Thick and thin histograms show the results of calculations with and without (pure liquid drop model) shell corrections in potential energy.

near-barrier collisions of ^{64}Ni and ^{136}Xe with a lead target exceed theoretical estimations. In both cases the calculated cross sections for the formation of heaviest trans-target nuclei in multinucleon transfer reactions (as well as in the reaction $^{160}\text{Gd} + ^{186}\text{W}$ discussed above) underestimate the corresponding experimental data by about one order of magnitude.

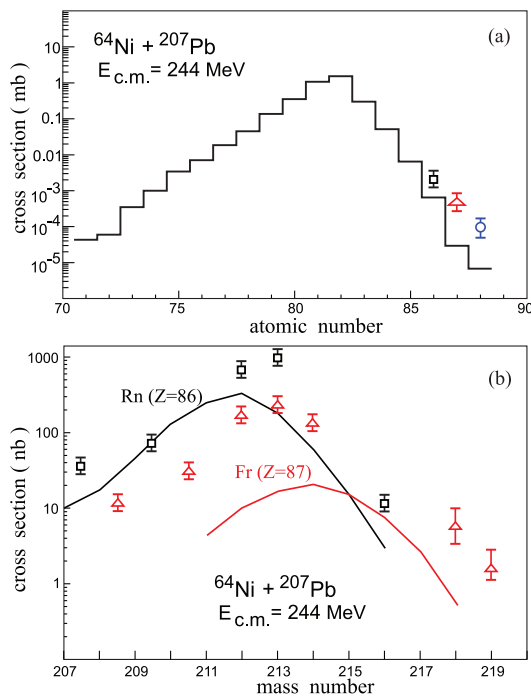


FIG. 4. (Color online) Charge distribution (a) and isotopic yields of Rn and Fr (b) in a forward angular window of $\pm 2^\circ$ in collisions of ^{64}Ni with a ^{207}Pb target at $E_{c.m.} = 244$ MeV. Experimental data [21] are shown by rectangles, triangles, and the circle, respectively, for Rn, Fr, and Ra isotopes.

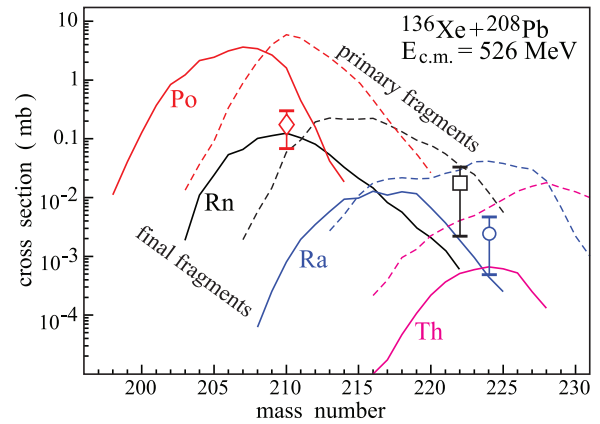


FIG. 5. (Color online) Cross sections integrated over the angular interval $40^\circ \leq \theta \leq 140^\circ$ (in accordance with experimental conditions) for the production of Po, Rn, Ra, and Th isotopes in the reaction $^{136}\text{Xe} + ^{208}\text{Pb}$ at $E_{c.m.} = 526$ MeV. Dashed curves show the yields of primary fragments. Experimental yields of ^{210}Po , ^{222}Rn , and ^{224}Ra [22] are shown, respectively, by the diamond, the rectangle, and the circle.

On the one hand, this means that formation of new neutron-enriched SH nuclei in low-energy collisions of ^{238}U with ^{248}Cm might be even more optimistic than predicted in Refs. [10,13]. On the other hand, available experimental data on the production of heavy trans-target nuclei in low-energy multinucleon transfer reactions (including those mentioned above) are still insufficient and fragmentary. This impedes improvement of the model to make more accurate predictions (especially in the SH mass area). Experiments of such kind are very difficult to perform due to the problems of on-line identification of heavy reaction products. Nevertheless, additional experimental data in this field are urgently needed not only for better estimations of SH element production but also for better understanding of the mechanisms of multinucleon transfers in low-energy collisions of very heavy ions and for experimental determination of such fundamental quantities of nuclear dynamics as nucleon transfer rate, nuclear viscosity, and so on (see below).

II. THE MODEL

Several models have been proposed and used for the description of mass transfer in deep inelastic heavy-ion collisions, namely, the Fokker-Planck [23] and master equations [24] for the corresponding distribution function, the Langevin equations [25], and more sophisticated semiclassical approaches [26–28]. The well-known GRAZING code [29] for describing nucleon transfer reactions in heavy-ion collisions is also available on the market (and recently it has become possible to run this code directly at the Nuclear Reaction Video (NRV) website [30]). The semiclassical model used by this code describes quite well few-nucleon transfer reactions (see, for example, the review paper [31]). However, multinucleon transfer processes cannot be described within this model; it

gives mass distributions of reaction fragments that are too narrow because the damped reaction channels with large kinetic energy loss are not included in the model.

Calculations performed within the microscopic time-dependent Schrödinger equations [32] have clearly demonstrated that, at low collision energies of heavy ions, nucleons do not “suddenly jump” from one nucleus to another. Instead, the wave functions of valence nucleons occupy two-center molecular states, spreading gradually over volumes of both nuclei. The same adiabatic low-energy collision dynamics of heavy ions was found also within time-dependent Hartree-Fock (TDHF) calculations [33,34]. This means that the perturbation models based on a calculation of the sudden overlapping of single-particle wave functions of transferred nucleons (in donor and acceptor nuclei, respectively) cannot be used for description of multinucleon transfer and quasi-fission processes in low-energy heavy-ion damped collisions. Indeed the two-center shell model and the adiabatic potential energy look most appropriate for the quantitative description of such processes.

A model based on the Langevin-type dynamical equations of motion was proposed recently [15,16] for simultaneous description of strongly coupled multinucleon transfer, quasi-fission, and fusion-fission reaction channels (which are difficult to distinguish experimentally in many cases). The distance between the nuclear centers, R (corresponding to the elongation of a mononucleus when it is formed), dynamic spheroidal-type surface deformations δ_1 and δ_2 , neutron and proton asymmetries, $\eta_N = (2N - N_{CN})/N_{CN}$ and $\eta_Z = (2Z - Z_{CN})/Z_{CN}$ (where N and Z are the neutron and proton numbers in one of the fragments, whereas N_{CN} and Z_{CN} refer to the whole nuclear system) are the most relevant degrees of freedom for the description of mass and charge transfer in deep inelastic scattering jointly with fusion-fission dynamics.

In low-energy damped collisions of heavy ions just the multidimensional potential energy surface regulates to a great extent the evolution of the nuclear system. In our approach we use a time-dependent potential energy, which after contact gradually transforms from a diabatic potential energy into an adiabatic one: $V(R, \delta_1, \delta_2, \eta_N, \eta_Z; t) = V_{\text{diab}}[1 - f(t)] + V_{\text{adiab}}f(t)$ [15]. Here t is the time of interaction and $f(t)$ is a smoothing function satisfying the conditions $f(t=0) = 0$ and $f(t \gg \tau_{\text{relax}}) = 1$, where τ_{relax} is an adjustable parameter $\sim 10^{-21}$ s.

The diabatic potential energy is calculated within the double-folding procedure at the initial reaction stage, whereas in the adiabatic reaction stage we use the extended version of the two-center shell model [35], the computational version of which can be found at the website listed in Ref. [36]. Note that the diabatic, V_{diab} , and adiabatic, V_{adiab} , potential energies depend on the same variables and they are equal to each other for well-separated nuclei. Thus, the total potential energy, $V(R, \delta_1, \delta_2, \eta_N, \eta_Z; t)$, is a quite smooth function of all the parameters, providing smooth driving forces, $-\partial V/\partial q_i$, at all reaction stages.

For all the variables, with the exception of the neutron and proton transfers, we use the usual Langevin equations of motion with the inertia parameters, μ_R and μ_δ , calculated

within the Werner-Wheeler approach [37]:

$$\frac{dq_i}{dt} = \frac{p_i}{\mu_i}, \quad \frac{dp_i}{dt} = \frac{\partial V_{\text{eff}}}{\partial q_i} - \gamma_i \frac{p_i}{\mu_i} + \sqrt{\gamma_i T} \Gamma_i(t). \quad (1)$$

Here q_i is one of the collective variables, p_i is the corresponding conjugate momentum, V_{eff} includes the centrifugal potential, $T = \sqrt{E^*/a}$ is the local nuclear temperature, $E^* = E_{\text{c.m.}} - V_{\text{eff}}(q_i; t) - E_{\text{kin}}$ is the excitation energy, γ_i is the appropriate friction coefficient, and $\Gamma_i(t)$ is a normalized random variable with a Gaussian distribution. The quantities γ_i , E^* , and T depend on the coordinates and, thus, on time (with all them evidently being equal to zero at the approaching reaction stage).

Nucleon exchange (nucleon rearrangement) can be described by the inertialess Langevin-type equations of motion derived from the master equations for the corresponding distribution functions [15]

$$\begin{aligned} \frac{d\eta_N}{dt} &= \frac{2}{N_{CN}} D_N^{(1)} + \frac{2}{N_{CN}} \sqrt{D_N^{(2)}} \Gamma_N(t), \\ \frac{d\eta_Z}{dt} &= \frac{2}{Z_{CN}} D_Z^{(1)} + \frac{2}{Z_{CN}} \sqrt{D_Z^{(2)}} \Gamma_Z(t). \end{aligned} \quad (2)$$

Here $D^{(1)}$ and $D^{(2)}$ are the transport coefficients. We assume that sequential nucleon transfers play a main role in mass rearrangement. In this case

$$\begin{aligned} D_{N,Z}^{(1)} &= \lambda_{N,Z}^{(+)}(A \rightarrow A+1) - \lambda_{N,Z}^{(-)}(A \rightarrow A-1), \\ D_{N,Z}^{(2)} &= \frac{1}{2} [\lambda_{N,Z}^{(+)}(A \rightarrow A+1) + \lambda_{N,Z}^{(-)}(A \rightarrow A-1)], \end{aligned} \quad (3)$$

where the macroscopic transition probabilities $\lambda_{N,Z}^{(\pm)}(A \rightarrow A' = A \pm 1)$ depend on the nuclear level density [23,24], $\lambda_{N,Z}^{(\pm)} = \lambda_{N,Z}^0 \sqrt{\rho(A \pm 1)/\rho(A)}$, and $\lambda_{N,Z}^0$ are the neutron and proton transfer rates. The nuclear level density $\rho \sim \exp(2\sqrt{aE^*})$ depends on the excitation energy E^* and, thus, the transition probabilities, $\lambda_{N,Z}^{(\pm)}$, are also coordinate- and time-dependent functions.

The first terms on the right-hand sides of Eqs. (2), $D_N^{(1)} \sim \partial V/\partial N$ and $D_Z^{(1)} \sim \partial V/\partial Z$, drive the system to the configuration with minimal potential energy in (Z, N) space, i.e., to the optimal Q value. The second terms in these equations, $\sim D_{N,Z}^{(2)}$, describe the diffusion of neutrons and protons in the system of overlapped nuclei.

For separated nuclei the nucleon exchange is still possible (though it is less probable) and has to be taken into account in Eqs. (2). We use the following final formula for the transition probabilities:

$$\lambda_{N,Z}^{(\pm)} = \lambda_{N,Z}^0 \sqrt{\frac{\rho(A \pm 1)}{\rho(A)}} P_{N,Z}^{tr}(R, A \rightarrow A \pm 1). \quad (4)$$

Here $P_{N,Z}^{tr}(R, A \rightarrow A \pm 1)$ is the probability of one-nucleon transfer (neutron or proton), which depends on the distance between the nuclear surfaces and the nucleon separation energy. This probability goes exponentially to zero at $R \rightarrow \infty$ and it is equal to unity for overlapping nuclei. A simple semiclassical formula [38] is used for the calculation of $P_{N,Z}^{tr}$. Thus, Eqs. (2)–(4) define a continuous change of charge and

mass asymmetries during the whole process (where, obviously, $d\eta_{N,Z}/dt \rightarrow 0$ for far separated nuclei).

The neutron and proton transfer rates, $\lambda_{N,Z}^0$, are the fundamental quantities of low-energy nuclear dynamics. However, their values are not well determined. For the first time the nucleon transfer rate, λ^0 , was estimated in Refs. [23,24] to be about 10^{22} s^{-1} . In our previous study we found that a value of $0.1 \times 10^{22} \text{ s}^{-1}$ for the nucleon transfer rate is quite appropriate to reproduce experimental data on the mass distributions of reaction products in several heavy-ion damped collisions [15,16]. However, this quantity is still rather uncertain. Its energy (and temperature) dependence has not yet been studied. A systematic analysis of experimental data on multinucleon transfer reactions at different collision energies is needed to determine the nucleon transfer rate more carefully. In our approach we distinguish the neutron and proton transfers (which is important for prediction of the yields of different isotopes of a given element).

At the approaching stage (for separated nuclei) the probabilities for neutron and proton transfers are different. The Coulomb barrier for protons leads to a faster decrease of their bound-state wave functions outside the nuclei, and, in general, $P_Z^r(R > R_1 + R_2, A \rightarrow A \pm 1) < P_N^r(R > R_1 + R_2, A \rightarrow A \pm 1)$. However, for well-overlapped nuclei single-particle motions of protons and neutrons are rather similar, and we assume that the neutron and proton transfer rates are equal to each other, i.e., $\lambda_N^0 = \lambda_Z^0 = \lambda^0/2$, and both are parameters of the model (i.e., they are not derived from some microscopic calculations). The model describes quite properly [39] the experimental difference in the cross sections of pure neutron and proton transfers [31].

Another rather uncertain quantity of low-energy nuclear dynamics is the nuclear friction (nuclear viscosity) responsible for the kinetic energy loss in heavy-ion damped collisions. A great interest in these processes was demonstrated 30 years ago. At that time, however, there was no appropriate theoretical model for obtaining an overall quantitative description of the available experimental data on the mass, charge, energy and angular distributions of reactions products. A number of different mechanisms to explain the energy loss in heavy-ion collisions have been suggested in the literature. A discussion of the subject can be found, e.g., in Refs. [40–43]. The uncertainty in the strength of the nuclear viscosity (as well as its form factor) is still large. Moreover, microscopic analysis shows that nuclear viscosity may also depend strongly on nuclear temperature [44].

For overlapping nuclei (mononucleus configuration) the two-body nuclear friction can be calculated within the Werner-Wheeler approach [37]. The corresponding viscosity coefficient μ_0 is estimated to be of the order of $10^{-23} \text{ MeV s fm}^{-3}$ [37,45]. The one-body dissipation mechanism [46,47] leads in general to even stronger nuclear friction. Note that in all the approaches the nuclear viscosity was found to be rather large, leading to so-called overdamped collision dynamics. For well-overlapped nuclei, kinetic energy in all degrees of freedom is rather low and the excited nuclear system creeps along the potential energy surface in multidimensional configuration space. For such overdamped dynamics the Langevin equations (1) are often reduced to the

Smoluchovski equations for q_i [42,48], which might be solved more easily (but in our calculations we do not use such a reduction).

The mass, energy, and angular distributions of binary reaction products depends strongly on the form factor (e.g., on the radius) of friction forces, and not so much on its strength. The strength parameter of nuclear friction (for separated nuclei) and its form factor are discussed in Refs. [15,16].

The double differential cross sections of all binary reaction channels are calculated as follows:

$$\frac{d^2\sigma_{N,Z}}{d\Omega dE}(E, \theta) = \int_0^\infty b db \frac{\Delta N_{N,Z}(b, E, \theta)}{N_{\text{tot}}(b)} \frac{1}{\sin(\theta)\Delta\theta\Delta E}. \quad (5)$$

Here $\Delta N_{N,Z}(b, E, \theta)$ is the number of events at a given impact parameter b in which a nucleus (N, Z) is formed in the exit channel with a kinetic energy in the region ($E, E + \Delta E$) and with a center-of-mass outgoing angle in the interval ($\theta, \theta + \Delta\theta$), and $N_{\text{tot}}(b)$ is the total number of simulated events for a given value of the impact parameter. This number depends strongly on the low level of the cross section which one needs to reach in calculation. For predictions of rare events with cross sections of $1 \mu\text{b}$ (primary fragments) one needs to test no fewer than 10^7 collisions (as many as in a real experiment).

Expression (5) describes the mass, charge, energy, and angular distributions of the *primary* fragments formed in the binary reaction. Subsequent de-excitation cascades of these fragments via emission of light particles and γ rays in competition with fission are taken into account explicitly for each event within the statistical model, leading to the *final* distributions of the reaction products. Parameters of this model can be found in Ref. [49], and all the decay widths can be calculated directly at the NRV website [50]. The sharing of the excitation energy between the primary fragments is assumed here to be proportional to their masses (which is also a debatable problem).

III. FORMATION OF TRANS-TARGET NUCLEI IN HEAVY-ION DAMPED COLLISIONS: TEST REACTIONS

Our model (formulated in Refs. [15,16] and briefly described above) was successfully used for a quantitative description of available experimental data on heavy-ion deep inelastic scattering and quasi-fission processes [15,16,39,51]. Rather satisfactory quantitative description of all experimental regularities of these reactions, namely, the mass, charge, energy, and angular distributions of reactions fragments, was obtained. Several predictions have been made within the model for the production of new neutron-rich heavy nuclei located along the closed neutron shell $N = 126$ [11] (the last waiting point in astrophysical nucleosynthesis) and in the SH mass area [39].

However, as mentioned above, a careful analysis of available and new experimental data demonstrates that our model probably underestimates the yields of reaction fragments with masses heavier than the target mass. In Fig. 6 the mass and charge distributions of reaction fragments formed in the $^{86}\text{Kr} + ^{166}\text{Er}$ [52] and $^{136}\text{Xe} + ^{208}\text{Pb}$ [22] collisions at $E_{\text{c.m.}} = 464$ and 526 MeV , correspondingly, are shown. In the

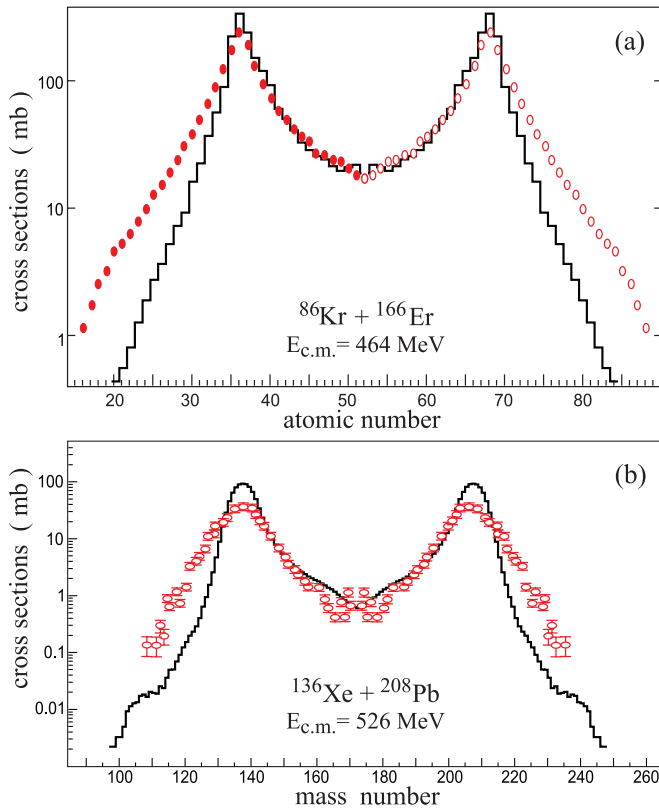


FIG. 6. (Color online) Charge and mass distribution of primary reaction fragments in the reactions $^{86}\text{Kr} + ^{166}\text{Er}$ [52] (a) and $^{136}\text{Xe} + ^{208}\text{Pb}$ [22] (b) at $E_{c.m.} = 464$ and 526 MeV, correspondingly (where open symbols on the right part of the upper plot are just the mirror reflection of the experimental data shown in the left part). The histograms indicate the calculations performed within the model described above.

case of the $^{86}\text{Kr} + ^{166}\text{Er}$ reaction only light (projectilelike) fragments were detected and the right part of the plot is drawn by assuming a binary reaction mechanism. For the $^{136}\text{Xe} + ^{208}\text{Pb}$ collision both fragments were detected in coincidence by the two-arm time-of-flight spectrometer [22] with a mass resolution of 7 units. Coincidence allows one to avoid contamination by fission fragments of excited targetlike nuclei.

As can be seen, the model describes quite well the yields of reaction fragments with intermediate masses $A_{\text{proj}} < A_1$, $A_2 < A_{\text{targ}}$, and it definitely underestimates the probability for the formation of reaction products with $A_1 < A_{\text{proj}}$ and $A_2 > A_{\text{targ}}$.

Note that the “mass antisymmetrization” (formation of $A_1 < A_{\text{proj}}$ and $A_2 > A_{\text{targ}}$) is energetically unfavorable for both systems. Q values become more and more negative with decreasing A_1 (and increasing A_2), whereas the production of intermediate masses ($A_{\text{proj}} < A_1$, $A_2 < A_{\text{targ}}$) is accompanied by close to zero or even positive Q values. In addition, this leads to a much sharper decrease of the calculated cross sections for the “antisymmetrizing” exit channels. However, in experiments this Q -value effect is less visible (see Fig. 6). Such an underestimation of the cross sections for the formation

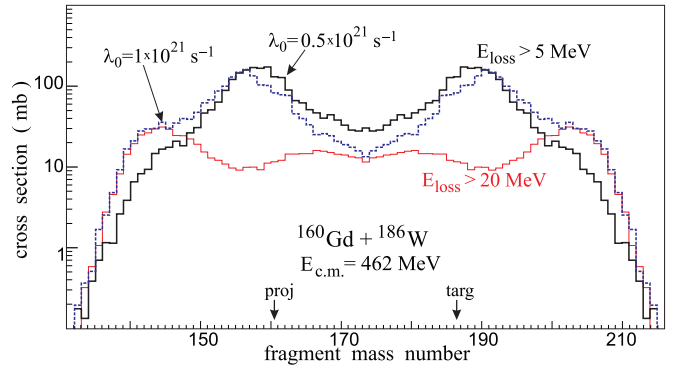


FIG. 7. (Color online) Calculated mass distributions of primary reaction fragments with total energy loss higher than 5 MeV formed in collisions of ^{160}Gd with ^{186}W at $E_{c.m.} = 462$ MeV depending on the value of the nucleon transfer rate: $\lambda_0 = 0.5 \times 10^{21} \text{ s}^{-1}$ (thick histogram); $\lambda_0 = 1 \times 10^{21} \text{ s}^{-1}$ (dotted histogram). Thin histogram shows the yield of fragments at $\lambda_0 = 1 \times 10^{21} \text{ s}^{-1}$ and total energy loss higher than 20 MeV.

of trans-target nuclei can be very important for planning future experiments on the production of neutron-rich isotopes of SH elements in multinucleon transfer reactions [17,18].

To improve the model and to adjust more carefully the values of some parameters (nucleon transfer rate, nuclear viscosity, and so on) we need to perform a more systematic analysis of the experimental data. Unfortunately, there are only scanty experimental data on the production of trans-target reaction fragments in low-energy damped collisions of heavy ions. As already mentioned, it is very difficult to perform such experiments especially with actinide targets because of the high fission probability of excited heavy reaction products. In this connection some surrogate reactions must be searched for and studied experimentally.

To study the shell effects leading to the enhanced yield of trans-target fragments (“antisymmetrizing” mass transfer) one needs to choose projectile-target combinations with nonmagic initial nuclei (not like the $^{136}\text{Xe} + ^{208}\text{Pb}$ reaction in which the nucleon diffusion dominates because the initial configuration is already located at the bottom of a deep potential valley due to high binding energies of these nuclei). One such combination, $^{160}\text{Gd} + ^{186}\text{W}$, was already proposed [19] and studied experimentally [20] (see above). In this system one neutron closed shell ($N = 82$) is located to the “left” of the projectile whereas the other ($N = 126$) is located to the “right” of the target on the fragment mass axis. Our calculations predicted an unusual mass distribution of reaction fragments in this reaction, and in the experiment it was found to be even more exotic: almost constant values of the cross section for formation of nuclei with $A > A_{\text{targ}}$ (see Fig. 3).

Unfortunately, as already mentioned, the experimental technique used did not allow one to measure the yields of stable and short-lived isotopes nor to see the total shape of the mass distribution. It is very desirable to repeat this experiment with on-line measurement of the mass (and probably charge) distribution.

In Fig. 7 the calculated reaction fragment mass distributions in collisions of ^{160}Gd with a ^{186}W target are shown depending

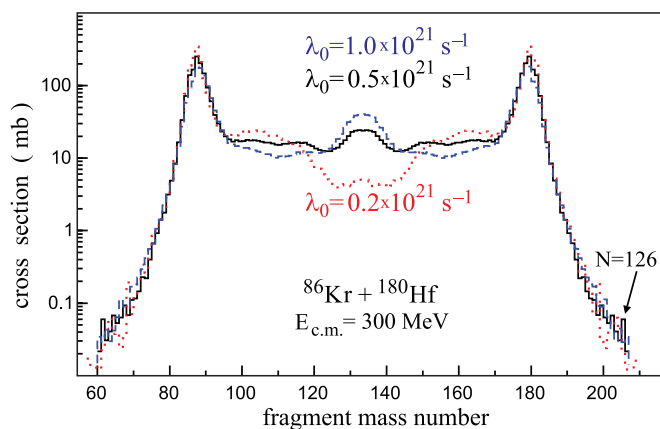


FIG. 8. (Color online) Mass distributions of primary reaction fragments with total energy loss higher than 10 MeV formed in collisions of ^{86}Kr with ^{180}Hf at $E_{c.m.} = 300$ MeV depending on the value of the nucleon transfer rate: $\lambda_0 = 0.2 \times 10^{21}$, 0.5×10^{21} , and $1.0 \times 10^{21} \text{ s}^{-1}$ (dotted, solid, and dashed histograms, correspondingly).

on the value of the nucleon transfer rate λ^0 . In contrast with $^{136}\text{Xe} + ^{208}\text{Pb}$, the mass distribution in this reaction is rather sensitive to the values of the model parameters, which, thus, could be adjusted more precisely from comparison with experimental data would they become available in a wide region of fragment masses. Note that in this case the mass distribution depends strongly on the experimental conditions. The yield of fragments with masses close to the projectile and target masses decreases by one order of magnitude if the quasielastic events with low energy loss ($E_{\text{loss}} < 20$ MeV) are excluded (see the thin histogram in Fig. 7).

The influence of the nucleon transfer rate on the mass distribution of reaction fragments in low-energy heavy-ion collisions is not so evident. In the case of $^{160}\text{Gd} + ^{186}\text{W}$ collision a larger value of the nucleon transfer rate leads to a wider mass distribution of reaction fragments with $A_1 < A_{\text{proj}}$ and $A_2 > A_{\text{targ}}$ (see Fig. 7). However, in other reactions just the yield of fragments with intermediate masses, $A_1 \sim A_2 \sim (A_{\text{proj}} + A_{\text{targ}})/2$, strongly depends on the value of this parameter (see the case of $^{86}\text{Kr} + ^{180}\text{Hf}$ collisions shown in Fig. 8). Thus, to derive more precisely the value of this fundamental parameter (including its temperature dependence) more experimental data are needed for several projectile-target combinations at several collision energies.

As already mentioned, such experiments are difficult to perform not only because of the low beam intensity of heavy projectiles but also because of the problem of identification of heavy (trans-target) reaction fragments. (On-line mass identification can be done by using the time-of-flight technique with an accuracy of several mass units, but for the moment there is no method for charge identification of such fragments.) Consequently, the decay properties of the final reaction fragments are often used for their identification (see, e.g., [20–22]).

In this connection, study of the multinucleon transfer reactions in which the trans-target reaction products are located

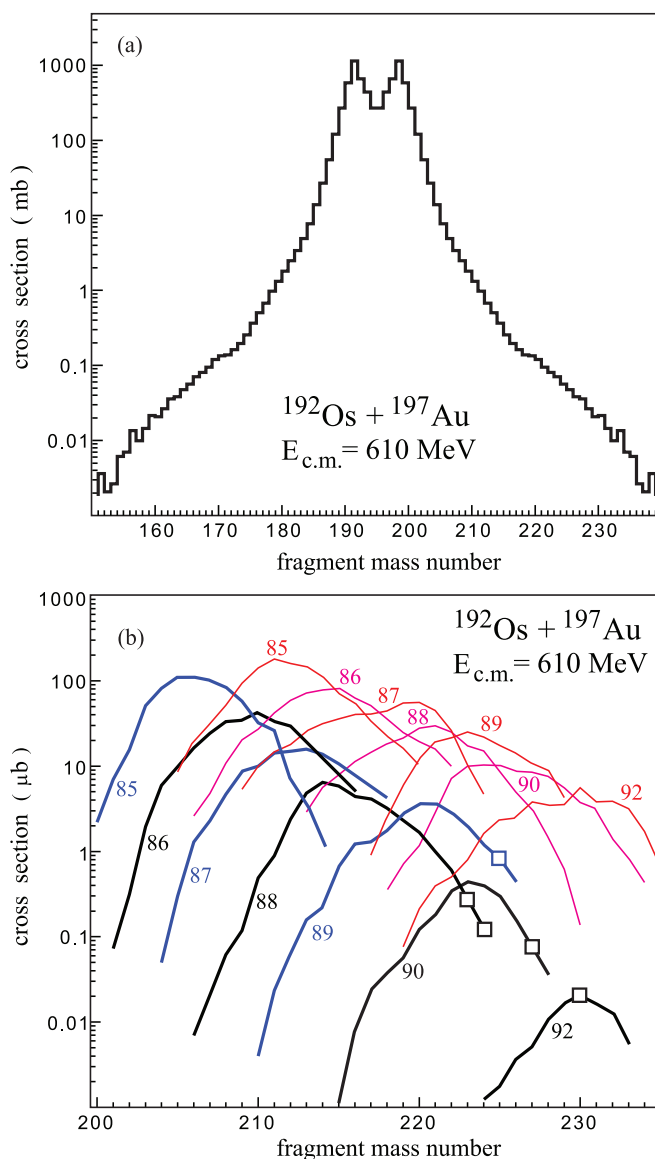


FIG. 9. (Color online) (a) Mass distributions of primary reaction fragments with total energy loss higher than 10 MeV formed in collisions of ^{192}Os with ^{197}Au at $E_{c.m.} = 610$ MeV. (b) The yields of isotopes of trans-target elements (with charge numbers near the curves) for primary nuclei (thin lines) and surviving nuclei (thick lines). The open rectangles show the reference-point α -decaying isotopes (with half-lives of several days), the yields of which can be measured in more easily realizable off-line experiments.

in the region of known α -decaying nuclei ($Z > 83$) may look quite appropriate. In Fig. 9 the estimated isotopic yields of heavy elements (from At to U) produced in the reaction $^{192}\text{Os} + ^{197}\text{Au}$ at $E_{c.m.} = 610$ MeV are shown. For most of these isotopes α decay dominates with well-known α lines. Both long-lived and short-lived α -decaying isotopes are there, and, thus, off-line and on-line identification of them are possible. As can be seen, one may expect to measure transfer up to 13 protons (more than 30 nucleons) to the target with the cross sections at the level of a few tens of nanobarns.

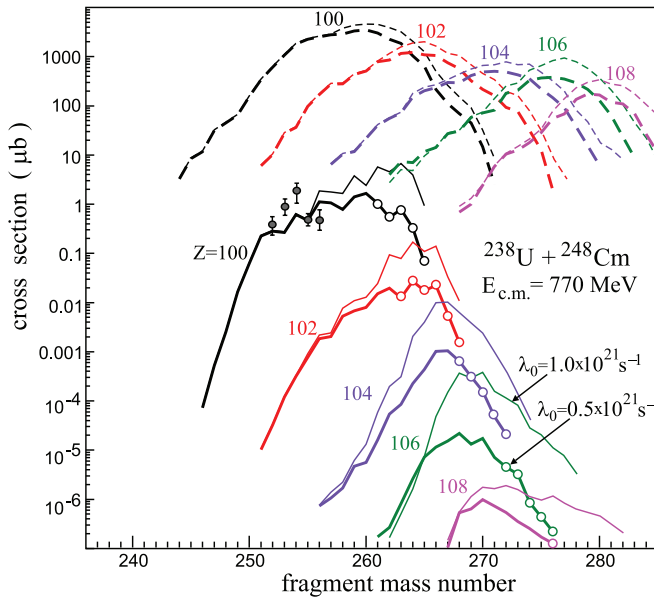


FIG. 10. (Color online) Cross sections for the production of transfermium nuclei in collisions of ^{238}U with a ^{248}Cm target at $E_{\text{c.m.}} = 770$ MeV calculated at the value of the nucleon transfer rate $\lambda_0 = 0.5 \times 10^{21} \text{ s}^{-1}$ (thick curves). Open circles indicate new isotopes of transfermium elements (with numbers near the curves). The dashed curves indicate the cross sections for the production of primary fragments. Thin lines show the result of calculations at $\lambda_0 = 1.0 \times 10^{21} \text{ s}^{-1}$. Experimental data are taken from Ref. [5] for the production of fermium isotopes in this reaction at beam energy $E_{\text{c.m.}} = 862$ MeV before beam enters the thick ^{248}Cm target.

IV. ACTINIDE BEAMS AND TARGETS

The use of actinide beams and/or actinide targets makes it possible to produce new neutron-enriched isotopes of transfermium elements located along the stability line and to the right of it, that is, in the unexplored area of the nuclear map. The most promising reaction is $^{238}\text{U} + ^{248}\text{Cm}$, which was already studied experimentally [5] and theoretically [12,13]. We performed a more careful analysis of this reaction by trying to determine the uncertainty of our predictions conditioned by the uncertainty in the values of some model parameters, such as proton and neutron transfer rates and nuclear viscosity (see above).

In Fig. 10 the results of our new calculations are shown for the formation of primary and surviving isotopes of some transfermium elements in the reaction $^{238}\text{U} + ^{248}\text{Cm}$ at a center-of-mass energy of 770 MeV. The obtained results are rather optimistic. As can be seen, new neutron-rich isotopes of transfermium elements with $Z = 100$ – 104 (located already at the stability line and beyond it) can be produced with cross sections of several hundreds of picobarns. The cross sections for the production of new neutron-rich isotopes of seaborgium and hassium ($Z = 106, 108$) are also higher than 1 pb. Note that the enhanced yield of primary trans-target nuclei with $A > 265$ in this reaction is conditioned just by the shell effects (see Fig. 1), namely, by decreasing the potential energy in the

channels with formation of projectilelike fragments close to the doubly magic nucleus ^{208}Pb .

Owing to the extremely low survival probability of excited heavy primary trans-target reaction fragments the cross sections for the production of SH nuclei located just in the middle of the island of stability ($Z \sim 112, N \sim 180$) were found to be less than 1 pb in this reaction [12,13]. This is too low to perform experiments aimed at the production of these nuclei at available facilities. However, as mentioned above, our model probably underestimates the yields of primary trans-target reaction fragments.

A rather unusual dependence of the calculated cross sections on the value of the nucleon transfer rate was found. Increasing this parameter by a factor of 2 leads to an increase (also by a factor of 2 or 3) only in the yields of neutron-enriched primary trans-target fragments (see the thin dashed curves in Fig. 10). At the same time, this leads to an increase in the yields of final (surviving) neutron-enriched isotopes of trans-target elements by more than one order of magnitude. This means that larger values of the nucleon transfer rate λ_0 may lead in this reaction to formation of less excited heavy trans-target nuclei at an earlier reaction stage (since a lower excitation energy means a higher survival probability and a smaller number of evaporated neutrons). As already mentioned, uncertainty in the values of nuclear friction parameters (responsible for the damping of relative motion kinetic energy) has a weaker impact on the yields of trans-target reaction fragments (because of the high strength of the nuclear viscosity). Additional uncertainty of the predictions for the formation of neutron-enriched transfermium nuclei in multinucleon transfer reactions arises from the uncertainty of their survival probability, which strongly depends on the fission barriers of these nuclei, which also cannot be estimated very accurately. Taken together these factors mean that at the moment one cannot make such predictions very precisely, so at least factor of 10 should be kept in mind.

The other combinations of actinide projectiles and targets can also be considered for future experiments on the production of new transuranium nuclei. In Fig. 11 the calculated cross sections are shown for the production of primary reaction fragments and fermium isotopes in damped collisions of ^{232}Th with several actinide targets, ^{238}U , ^{244}Pu , and ^{248}Cm . The collision energies were adjusted in such a way that for all three cases they exceed by about 10 MeV the corresponding potential energies of contact (tip-to-tip) configurations of colliding nuclei with ground-state deformations. Note that this contact potential energy may decrease afterward owing to dynamic deformations of both nuclei and nucleon rearrangement with positive Q values (leading thus to a further increase of nuclear temperature).

As can be seen, the cross sections for the production of the heaviest trans-target primary fragments with $A \sim 280$ are more or less equal for all these reactions [see Fig. 11(a)]. However, the yield of neutron-enriched fermium isotopes with $A > 260$ is higher in the $^{232}\text{Th} + ^{248}\text{Cm}$ reaction, for which it is quite comparable or even higher than in the $^{238}\text{U} + ^{248}\text{Cm}$ reaction. Note that the off-line detection of α -decaying ^{255}Fm ($T_{1/2} = 20$ h, populated by β^- decay of ^{255}Es with

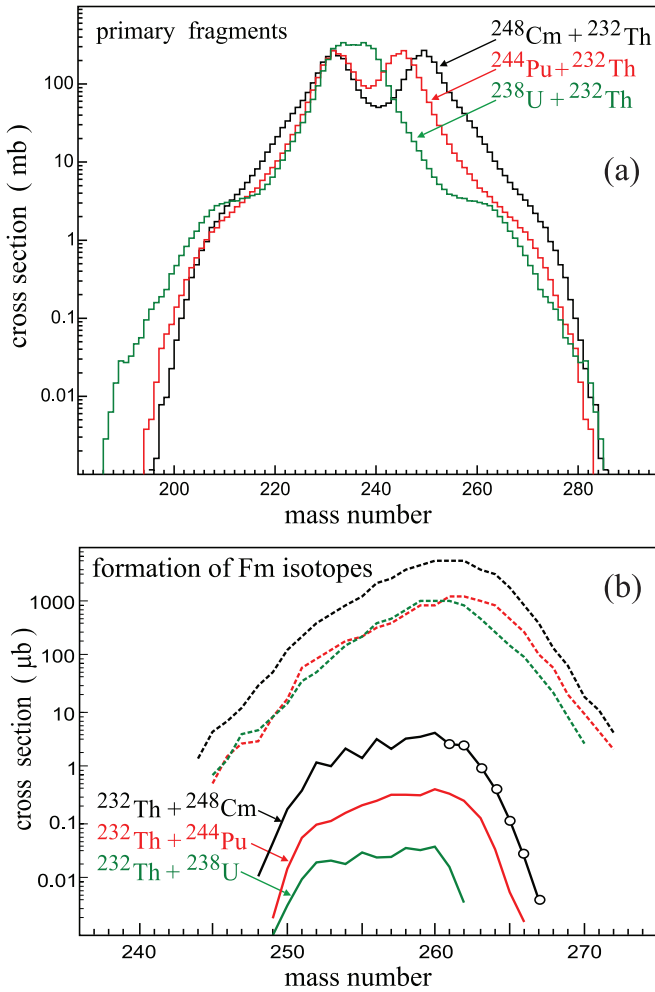


FIG. 11. (Color online) Mass distribution (a) and isotopic yields of fermium nuclei (b) in collisions of ^{232}Th with ^{238}U , ^{244}Pu , and ^{248}Cm at $E_{c.m.} = 715$, 730 , and 750 MeV, correspondingly ($\lambda_0 = 0.5 \times 10^{21} \text{ s}^{-1}$). Dashed curves in (b) indicate isotopic yields of primary (excited) fermium nuclei and open circles show new isotopes.

$T_{1/2} = 39.8$ d), ^{257}Fm ($T_{1/2} = 100.5$ d), and ^{258}Md ($T_{1/2} = 51.5$ d) can be used as a good benchmark for all these transfer reactions.

Actinide beams (as well as actinide targets) might be successfully used also for the production of new neutron-rich nuclei around the closed neutron shell $N = 126$, the region having the largest impact on the astrophysical r-process. Near-barrier collisions of ^{136}Xe and ^{192}Os with a ^{208}Pb target were predicted to be quite promising for the production of new nuclei with $N \sim 126$ [11,13]. The corresponding cross sections were found to be about $1 \mu\text{b}$ and less. The use of heavy radioactive ion beams (such as ^{132}Sn [13] or ^{154}Xe [53]) gives a gain in the nucleon transfer cross sections but not in the final yields of new neutron-rich nuclei because of the low intensity of these beams.

Low-energy collisions of stable neutron-rich isotopes of elements located below lead (such as ^{192}Os or ^{198}Pt) with available actinide nuclei look more favorable for the production and study of new neutron-rich nuclei located around the neutron closed shell $N = 126$. The distribution of primary

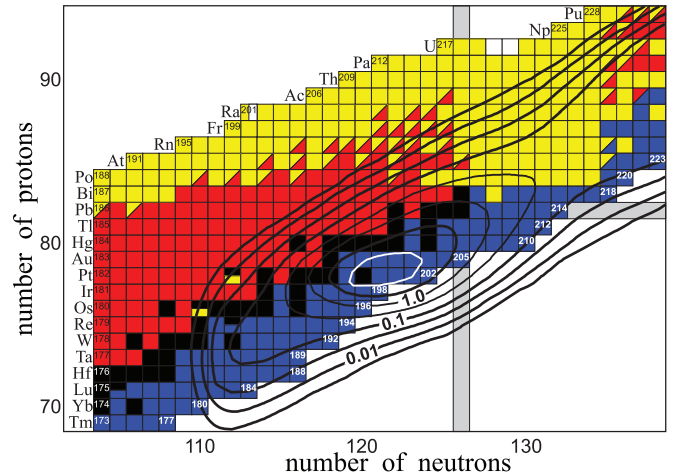


FIG. 12. (Color online) Contour plot of the cross sections (on a logarithmic scale) for the formation of primary reaction fragments in collisions of ^{198}Pt with ^{238}U at $E_{c.m.} = 700$ MeV. Contour lines are drawn over half an order of magnitude and the units of measurement are shown in millibarns.

fragments formed in transfer reactions is concentrated around the line connecting the projectile and the target (just due to conservation of proton and neutron numbers). If one reaction partner has a neutron excess (such as ^{238}U), then this line will be inclined to the neutron axis. The distribution of primary fragments in the (Z, N) plane is shown in Fig. 12 for the case of transfer reaction products formed in low-energy collisions of ^{198}Pt with ^{238}U at $E_{c.m.} = 700$ MeV. As can be seen a lot of new isotopes in the region of the closed neutron shell $N = 126$ can be synthesized in this reaction.

Estimated cross sections for the production of the final (surviving) isotopes of the elements with $Z = 71-78$ in low-energy collisions of ^{198}Pt with ^{238}U are shown in Fig. 13. On average,

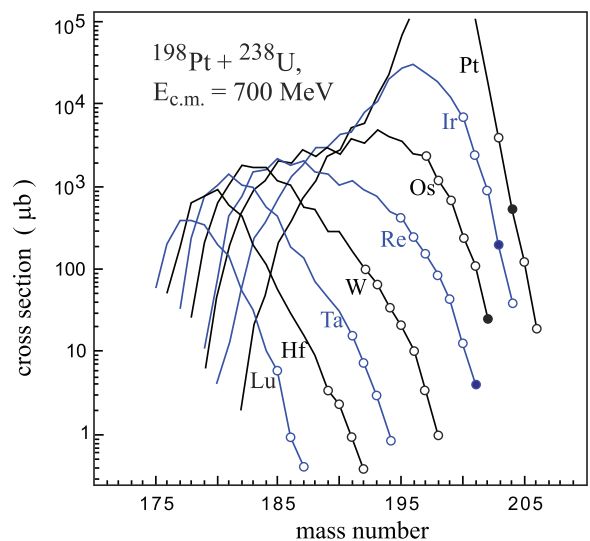


FIG. 13. (Color online) Isotopic yields of elements below lead (from Lu to Pt) in collisions of ^{198}Pt with ^{238}U at $E_{c.m.} = 700$ MeV. Circles denote not-yet-known isotopes (with solid circles showing isotopes with the closed neutron shell $N = 126$).

the cross sections for the production of new neutron-rich heavy nuclei (including those located along the closed neutron shell $N = 126$) in this reaction are higher than in collisions of ^{136}Xe or ^{192}Os with a ^{208}Pb target [13] (though a contamination by uranium fission fragments probably may reduce this gain in the cross sections).

V. CONCLUSION

Low-energy multinucleon transfer reactions look quite appropriate for the production of new neutron-enriched heavy nuclei. Reactions with actinide beams and targets are of special interest for synthesis of new neutron-enriched superheavy nuclei and not-yet-known nuclei with the closed neutron shell $N = 126$ having the largest impact on the astrophysical r -process. However, it is rather difficult to perform these experiments because of the low beam intensities of the massive projectiles and problems with separating and detecting the heavy reaction products. In this connection, realistic predictions of the corresponding cross sections for different projectile-target combinations are definitely required.

The estimated cross sections for the production of new neutron-enriched heavy nuclei in low-energy multinucleon transfer reactions are found to be very promising (see,

for example, the case of $^{198}\text{Pt} + ^{238}\text{U}$) for planning such experiments at currently available accelerators. Unfortunately, some uncertainty remains in the values of several parameters used in the calculations. This uncertainty does not allow one to perform very accurate predictions for the productions of new (especially trans-target) nuclei in multinucleon transfer reactions. Most of these model parameters (nucleon transfer rate, nuclear viscosity, and fission barriers) are fundamental characteristics of low-energy nuclear dynamics. Determination of the values of these parameters (as well as their temperature dependence) is of significance in its own right. The available experimental data on the production of heavy nuclei in low-energy multinucleon transfer reactions are still insufficient and fragmentary. Urgently needed are new experiments, including those in which the role of shell effects in reaction dynamics can be clarified. Careful experimental study of the mass distributions in damped collisions of ^{160}Gd with ^{186}W or ^{192}Os with ^{197}Au (a kind of surrogate reaction) could be quite useful.

ACKNOWLEDGMENT

We are indebted to the DFG-RFBR Collaboration for support of our studies.

-
- [1] E. K. Hulet *et al.*, *Phys. Rev. Lett.* **39**, 385 (1977).
 - [2] M. Schädel *et al.*, *Phys. Rev. Lett.* **41**, 469 (1978).
 - [3] H. Essel, K. Hartel, W. Henning, P. Kienle, H. J. Körner, K. E. Rehm, P. Sperr, W. Wagner, and H. Spieler, *Z. Phys. A* **289**, 265 (1979).
 - [4] H. Freiesleben, K. D. Hildenbrand, F. Pühlhofer, W. F. W. Schneider, R. Bock, D. V. Harrach, and H. J. Specht, *Z. Phys. A* **292**, 171 (1979).
 - [5] M. Schädel *et al.*, *Phys. Rev. Lett.* **48**, 852 (1982).
 - [6] K. J. Moody, D. Lee, R. B. Welch, K. E. Gregorich, G. T. Seaborg, R. W. Loughheed, and E. K. Hulet, *Phys. Rev. C* **33**, 1315 (1986).
 - [7] R. B. Welch, K. J. Moody, K. E. Gregorich, D. Lee, and G. T. Seaborg, *Phys. Rev. C* **35**, 204 (1987).
 - [8] W. Mayer, G. Beier, J. Friese, W. Henning, P. Kienle, H. J. Körner, W. A. Mayer, L. Müller, G. Rosner, and W. Wagner, *Phys. Lett. B* **152**, 162 (1985).
 - [9] V. I. Zagrebaev, A. V. Karpov, I. N. Mishustin, and W. Greiner, *Phys. Rev. C* **84**, 044617 (2011).
 - [10] V. I. Zagrebaev, Yu. Ts. Oganessian, M. G. Itkis, and W. Greiner, *Phys. Rev. C* **73**, 031602 (2006).
 - [11] V. Zagrebaev and W. Greiner, *Phys. Rev. Lett.* **101**, 122701 (2008).
 - [12] V. I. Zagrebaev and W. Greiner, *Phys. Rev. C* **78**, 034610 (2008).
 - [13] V. I. Zagrebaev and W. Greiner, *Phys. Rev. C* **83**, 044618 (2011).
 - [14] M. G. Itkis *et al.*, *Nucl. Phys. A* **734**, 136 (2004).
 - [15] V. Zagrebaev and W. Greiner, *J. Phys. G* **31**, 825 (2005).
 - [16] V. Zagrebaev and W. Greiner, *J. Phys. G* **34**, 1 (2007).
 - [17] GSI workshops on Inelastic Reaction Isotope Separator for Heavy Elements, <http://www-win.gsi.de/iris-fall-2010/>.
 - [18] A. Drouart *et al.*, *Nucl. Phys. A* **834**, 747 (2010).
 - [19] V. Zagrebaev and W. Greiner, *J. Phys. G* **34**, 2265 (2007).
 - [20] W. Loveland, A. M. Vinodkumar, D. Peterson, and J. P. Greene, *Phys. Rev. C* **83**, 044610 (2011).
 - [21] S. Heinz (private communication).
 - [22] E. M. Kozulin *et al.*, *Phys. Rev. C* **86**, 044611 (2012).
 - [23] W. Nörenberg, *Phys. Lett. B* **52**, 289 (1974).
 - [24] L. G. Moretto and J. S. Sventek, *Phys. Lett. B* **58**, 26 (1975).
 - [25] P. Fröbrich and S. Y. Xu, *Nucl. Phys. A* **477**, 143 (1988).
 - [26] E. Vigezzi and A. Winther, *Ann. Phys. (NY)* **192**, 432 (1989).
 - [27] V. I. Zagrebaev, *Ann. Phys. (NY)* **197**, 33 (1990).
 - [28] A. Winther, *Nucl. Phys. A* **594**, 203 (1995).
 - [29] <http://personalpages.to.infn.it/~nanni/grazing/>.
 - [30] <http://nr.v.jinr.ru/nrv/webnrv/grazing/>.
 - [31] L. Corradi, G. Pollarolo, and S. Szilner, *J. Phys. G* **36**, 113101 (2009).
 - [32] V. I. Zagrebaev, V. V. Samarin, and W. Greiner, *Phys. Rev. C* **75**, 035809 (2007).
 - [33] A. S. Umar, V. E. Oberacker, and J. A. Maruhn, *Eur. Phys. J. A* **37**, 245 (2008).
 - [34] C. Simenel, A. Wakhle, and B. Avez, NN2012 conference, San Antonio, Texas, 2012 (to be published in JPCS).
 - [35] V. Zagrebaev, A. Karpov, Y. Aritomo, M. Naumenko, and W. Greiner, *Phys. Part. Nucl.* **38**, 469 (2007).
 - [36] V. Zagrebaev, A. Alekseev, A. Denikin, A. Karpov, and V. Samarin, Two Center Shell Model code of NRv, <http://nr.v.jinr.ru/nrv/>.
 - [37] F. G. Werner and J. A. Wheeler (private communication); K. T. R. Davies, A. J. Sierk, and J. R. Nix, *Phys. Rev. C* **13**, 2385 (1976).
 - [38] V. I. Zagrebaev, *Phys. Rev. C* **67**, 061601 (2003).
 - [39] V. Zagrebaev and W. Greiner, *J. Phys. G* **35**, 125103 (2008).
 - [40] R. Bass, in *Nuclear Reactions with Heavy Ions* (Springer-Verlag, New York, 1980), p. 326.

- [41] W. U. Schröder and J. R. Huizenga, in *Treatise on Heavy-Ion Science*, edited by D. A. Bromley, Vol. 2 (Plenum, New York, 1984), p. 140.
- [42] Y. Abe, S. Ayik, P.-G. Reinhard, and E. Suraud, *Phys. Rep.* **275**, 49 (1996).
- [43] P. Fröbrich and I. I. Gonchar, *Phys. Rep.* **292**, 131 (1998).
- [44] H. Hofmann, *The Physics of Warm Nuclei* (Oxford University Press, Oxford, 2008).
- [45] K. T. R. Davies, R. A. Managan, J. R. Nix, and A. J. Sierk, *Phys. Rev. C* **16**, 1890 (1977).
- [46] J. Randrup and W. J. Swiatecki, *Nucl. Phys. A* **429**, 105 (1984).
- [47] H. Feldmeier, *Rep. Prog. Phys.* **50**, 915 (1987).
- [48] C. W. Gardiner, *Stochastic Methods* (Springer-Verlag, Berlin, 1990).
- [49] V. I. Zagrebaev, Y. Aritomo, M. G. Itkis, Yu. Ts. Oganessian, and M. Ohta, *Phys. Rev. C* **65**, 014607 (2001).
- [50] V. Zagrebaev, A. Alekseev, A. Denikin, A. Karpov, and V. Samarin, Statistical Model code of NRV, <http://nrv.jinr.ru/nrv/>.
- [51] Y. Aritomo, *Phys. Rev. C* **80**, 064604 (2009).
- [52] A. Gobbi, U. Lynen, A. Olmi, G. Rudolf, and H. Sann, in *Proceedings of the International School of Physics "Enrico Fermi," Course LXXVII, Varenna on Lake Como, Villa Monastero, 9th–21st July 1979* (North-Holland, Amsterdam, 1981), p. 1.
- [53] C. H. Dasso, G. Pollarolo, and A. Winther, *Phys. Rev. Lett.* **73**, 1907 (1994).